

Adsorption of K on Si(100) 2×1 at room temperature studied with photoelectron spectroscopy

Y.-C. Chao

Department of Physics and Measurement Technology, Linköping Institute of Technology, S-581 83 Linköping, Sweden

L. S. O. Johansson

Department of Synchrotron Radiation Research, Institute of Physics, University of Lund, Sölvegatan 14, S-223 62 Lund, Sweden

C. J. Karlsson, E. Landemark, and R. I. G. Uhrberg

Department of Physics and Measurement Technology, Linköping Institute of Technology, S-581 83 Linköping, Sweden

(Received 20 January 1995)

Different coverages of K on the Si(100) 2×1 surface were studied by photoelectron spectroscopy up to saturation coverage. The K $3p$ spectra show two components for coverages larger than 50% of saturation, which is consistent with the double-layer model. The Si $2p$ spectrum at saturation coverage shows a strong, well-resolved, K-induced component, with an energy shift of ~ 0.42 eV, toward lower binding energies. Based on its intensity and the 2×1 periodicity observed by low-energy electron diffraction (LEED) this component is assigned to Si atoms forming symmetric dimers on the surface. An abrupt decrease of the band bending at the surface of the n -type sample by ~ 0.23 eV, accompanied by the appearance of a surface state peak at the Fermi level, was observed for the initial growth. This peak is interpreted as due to a partial occupation of an empty surface band existing already for the clean surface. The smeared out appearance of the Si $2p$ core-level spectra for the smaller K exposures indicates that multiple surface shifts due to an inhomogeneous surface are present. For a coverage of about 30% of the saturation coverage, a sharpening of the line shape of the Si $2p$ spectra occurred and a 2×3 LEED pattern was observed, implying an ordering of the surface. At saturation coverage, another abrupt energy shift of the spectra, by ~ 0.2 eV, occurred toward higher binding energies. This shift coincides with a metallization of the surface, which has been reported in inverse and direct photoemission studies.

I. INTRODUCTION

Alkali-metal adsorption on semiconductor surfaces is presently a subject of widespread interest in surface science.¹ Due to the simple electronic structure and the chemically active nature, alkali-metal overlayers have been regarded as model systems for metal-semiconductor interfaces. We here concentrate on potassium adsorption on the Si(100) 2×1 surface which has been studied extensively both experimentally and theoretically but still is a matter of controversy. No consensus has been reached even on the most basic questions such as the room-temperature saturation coverage, the metallization of the substrate and/or the overlayer, the nature of the Si-K bonding, the surface morphology, and electronic structure.²

In an early study on the Si(100) 2×1 -Cs system Levine proposed a one-dimensional alkali-metal chain model.³ In this model alkali atoms form linear chains on top of the dimer rows of the substrate. The room-temperature saturation coverage, θ_s , is 0.5 ML for the Levine model [1 ML is defined as 6.78×10^{14} atoms per cm^2 , i.e., the surface atomic density of a truncated Si(100) 1×1 surface], which should result in a metallic surface with a half-filled π^* band. In contrast to what is expected for the Levine model, Enta *et al.*⁴ concluded from their angle-resolved photoemission data that the Si(100) 2×1 -K surface was semiconducting. Another model was proposed by Abukawa and Kono⁵ from a subsequent x-ray photoelec-

tron diffraction (XPD) study. In this so called double-layer model, shown in Fig. 1, K atoms are located both between and on top of the dimer rows, which gives a room temperature θ_s of 1 ML. After the work by Enta *et al.*⁴ and Abukawa and Kono,⁵ the double-layer model has been supported by several experimental investigations and theoretical calculations.⁶⁻¹² Recently, Kobayashi *et al.*¹¹ and Morikawa *et al.*¹⁰ used the optimized (2×1) asymmetric dimer structure as a starting configuration of the Si(100) substrate and performed a calculation by the first-principle molecular-dynamics method. They found that the most stable adsorption site at a coverage of 0.5 ML turned out to be the position above the third Si layer and between the Si dimer rows. Their theoretically optimized structure for a saturation coverage of 1 ML supports the double-layer model, in which K atoms occupy the sites above the third Si layer, both on and between the Si dimer rows.

The saturation coverage at room temperature is, however, still controversial. From an Auger electron diffraction (AED) study, Asensio *et al.*¹³ found that the adsorption position and the θ_s of K atoms depend strongly on the substrate temperature. Later Michel *et al.*² concluded by using Xe titration and photoelectron spectroscopy that a double-layer structure is not completed at room temperature. Riffe *et al.*¹⁴ performed a core-level photoemission experiment, from which a room temperature θ_s of 0.7 ML was derived. In recent STM (scanning tunneling microscopy) studies, Effner *et al.*¹⁵ and Brodde,

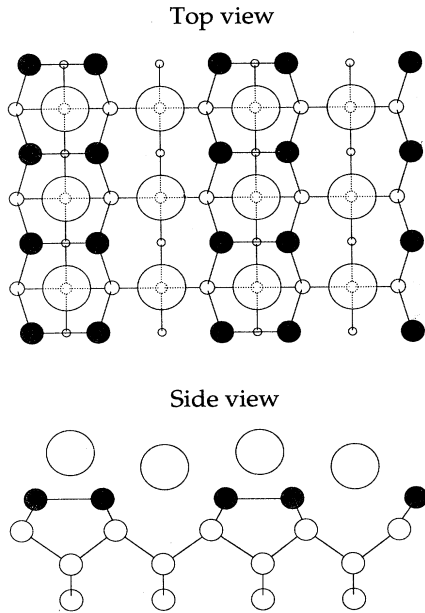


FIG. 1. Schematic illustration of the double-layer model for the Si(100) 2×1 -K surface as proposed in Ref. 5. K atoms (large shaded circles) are located both between and on top of the Si dimer rows (small shaded circles) right above the third Si layer (small dashed circles). For a clean Si(100) 2×1 surface, the Si atoms of the topmost layer form asymmetric dimers as shown in the inset in Fig. 6(a).

Bertrams, and Neddermeyer¹⁶ observed a metallic two-dimensional K layer with a θ_s of 1 ML. On the other hand, Soukiasian *et al.*¹⁷ suggested a room temperature θ_s of 0.5 ML based on the observation of K atoms forming one-dimensional chains parallel to the Si dimer rows, 7.68 Å apart, with a single adsorption site. All three STM investigations as well as the inverse and direct photoemission study by Johansson and Reihl¹² suggest a metallic character of the K-saturated surface.

For submonolayer coverages, Hashizume and co-workers^{18,19} found that for a coverage of ~ 0.02 – 0.05 ML, the K atoms first reside on top and over two neighboring Si dimer atoms in an off-center position, followed by an ordering in lines perpendicular to the dimer rows for increasing coverage. Observations of a disordered adlayer for small coverages and a 2×3 surface reconstruction for $\sim \frac{1}{3}$ ML were also done by STM and low-energy electron diffraction (LEED) studies.^{15,16,20} The nature of the bond between the K and the Si atoms was investigated recently by Souda *et al.*^{21,22} using a low-energy ion-scattering method. They concluded that the K-Si bond is ionic for a K coverage of ≤ 0.25 ML.

In order to further understand this system we have studied K adsorption on Si(100) for different coverages with high-resolution core-level spectroscopy and angle-resolved photoemission. A series of core-level and valence-band spectra of the Si(100) surface for increasing K coverages was obtained. Our high-resolution Si $2p$ core-level spectra provide much more information than earlier reports in the literature which allows us to address

some of the controversies about the Si(100) 2×1 -K system. Comparisons with other studies are also made in this paper.

II. EXPERIMENTAL DETAILS

The core-level photoemission experiment was performed at the MAX synchrotron radiation facility in Lund, Sweden. All core-level spectra shown in this paper were obtained by using a modified SX-700 plane grating monochromator and a large hemispherical electron-energy analyzer. The total energy resolution for the core-level data was < 70 meV and the angular acceptance of the analyzer was $\pm 8^\circ$. The angle-resolved photoelectron spectroscopy (ARPES) study was performed in Linköping at a photon energy of 21.2 eV with angular and energy resolutions better than $\pm 1^\circ$ and 150 meV, respectively. The base pressures of the vacuum chambers in the two experimental setups were $(1-2)\times 10^{-10}$ Torr.

An *n*-type, mirror polished, Si(100) single crystal ($\rho=2$ Ωcm , P) was preoxidized using an etching method²³ and cleaned *in situ* by stepwise heating up to $\sim 900^\circ\text{C}$, which resulted in a sharp two-domain 2×1 LEED pattern.²⁴

Potassium was evaporated from a well-outgassed getter source (SAES Getters) onto the samples at room temperature. The pressure increased less than 3×10^{-10} Torr during the exposures. The coverage of potassium was monitored by measuring the change in the work function $\Delta\Phi$. K-adsorbed samples for both the core-level and ARPES experiments were prepared every hour. There was no sign of oxidation in the valence-band spectra within this time period. The K atoms were always deposited onto a fresh Si(100) 2×1 surface obtained by annealing at $\sim 900^\circ\text{C}$ for 30 sec. The K exposures were repeated several times with excellent reproducibility of the data.

III. RESULTS AND DISCUSSION

Figure 2 shows a series of Si $2p$ core-level spectra recorded at a photon energy of 130 eV. All spectra are normalized to have the same integrated emission intensity. The lowermost spectrum, which was obtained from the clean Si(100) 2×1 surface, exhibits a prominent peak Su at the low binding-energy side which corresponds to the up atoms of asymmetric dimers (0.5 ML).²⁵ Spectra 2(a)–2(f) were recorded for surfaces that were exposed to an increasing amount of potassium. The work-function change $\Delta\Phi$ was used to monitor the potassium coverage. Already a coverage of a few percent of a monolayer, $\sim 4\%$ of saturation coverage, results in a considerable broadening of the Si $2p$ spectrum 2(a). There is also an abrupt shift to higher binding energies by ~ 0.23 eV, which corresponds to a change in the band bending. As $\Delta\Phi$ reached -2.65 eV, the Si $2p$ spectrum became sharper again. The coverage at this stage is about $\frac{1}{3}$ of θ_s . From spectra 2(a)–2(e) we observe a continuous shift of the spectra by 0.37 eV toward lower binding energies for increasing coverages. Close to saturation coverage a second abrupt shift to higher binding energy by ~ 0.2 eV occurred implying that the Fermi level moved closer to

the valence-band edge by this amount. At saturation coverage a strong, well-resolved, surface component *S* is the dominating feature in spectrum 2(f). The intensity of the surface component *S*, compared to the rest of the spectrum, is approximately twice that of *Su* for the clean surface.

K 3*p* core-level spectra recorded with a photon energy of 130 eV are shown in Fig. 3 for the same Si(100)-K surfaces as in Fig. 2. All spectra are here normalized with respect to the incident photon flux. The spectra were decomposed by a least-squares fitting procedure. An integrated background was used and the spin-orbit split, branching ratio, and Lorentzian width were 0.24 eV, 0.5,

and 0.14 eV [full width at half maximum (FWHM)], respectively. An increased singularity index (Doniach-Sunjić line shape) from zero for spectra (a) and (b) up to 0.065 with increasing K coverages is required to obtain the best fits. A second component (dotted line) appeared in spectra 3(d)–3(f), which provides evidence for at least two different adsorption sites. The energy separation between components *A* and *B* was ~ 0.46 eV near saturation coverage and the Gaussian width is 0.57 eV (FWHM) for both of them. The binding energy of the K 3*p* core level shows a variation with coverage consistent with that observed for the Si 2*p* core level. K 3*p* spectra were also recorded with photon energies of 100 and 70 eV and the spectra show very similar results in all three cases.

The integrated K 3*p* intensity versus exposure time is

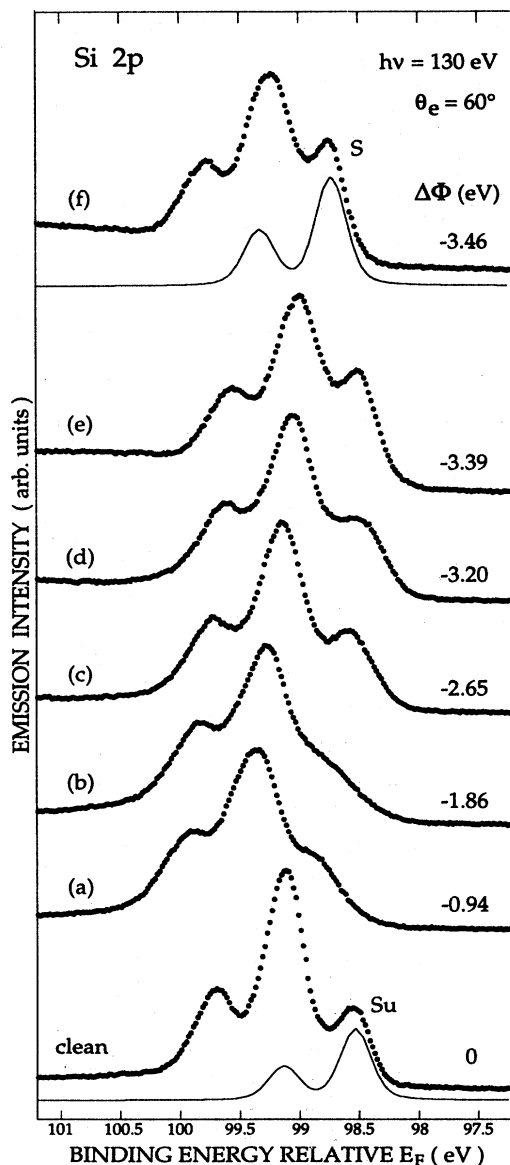


FIG. 2. Si 2*p* core-level spectra recorded with a photon energy of 130 eV at 60° emission angle for increasing K coverage. The coverage was determined indirectly by measuring the work-function change.

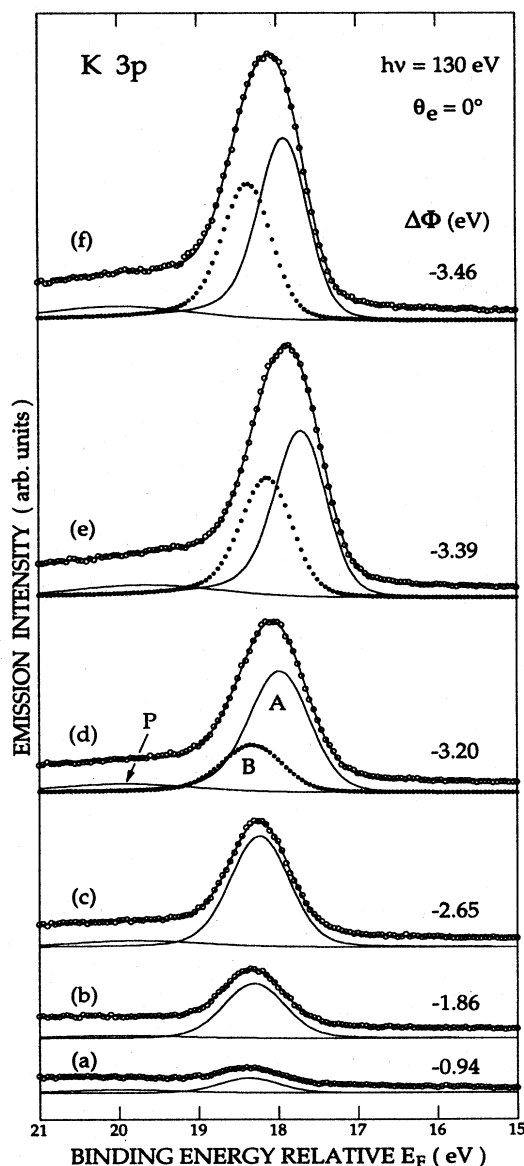


FIG. 3. A series of fitted K 3*p* core-level spectra recorded at normal emission from the same Si(100)-K surfaces as in Fig. 2.

shown in Fig. 4. The data points corresponding to spectra (a)–(f) in Fig. 3 are labeled. The total K 3*p* intensity, solid circles, increased linearly with the exposure time until it reached a constant value at ~ 8 min. This curve is consistent with the observations made from the K 3*p* spectra by Riffe *et al.*¹⁴ and Effner *et al.*¹⁵ but it is different from the curve obtained by Soukiassian *et al.*¹⁷ which showed no saturation when the pressure increase was in the 10^{-10} Torr range during exposure. The crosses and the triangles correspond to the integrated intensities of components A and B in the K 3*p* spectra in Fig. 3, respectively. As shown in Fig. 4, evidence for two different binding energies of the K 3*p* electrons indicating different adsorption sites is observed for coverages $\geq 0.5\theta_s$. For those coverages the component of the K 3*p* spectra at the higher binding energy B increases much faster with exposure time than component A. Some STM images^{15,16} show that most of the K atoms are preferentially adsorbed on trough sites (i.e., sites between dimer rows) for small coverages at which the surface has not yet reached the 2×3 reconstruction. The images of the 2×3 reconstructed surface show K atoms sitting on one specific trough site. For coverages larger than that corresponding to the 2×3 reconstruction, evidence for a second K site is clearly observed. The results of the K 3*p* core-level spectra agree quite well with the STM studies if one assigns the solid and dotted components in Fig. 3 to K atoms in “trough” and “top” sites, respectively. A third broad component P is also present in Fig. 3 which shows a slight increase in the intensity (open circles in Fig. 4) with increasing coverage. This component may be the result of a combination of a Si valence-band plasmon loss¹⁴ and a plasmon loss related to the K-Si interface. The energy location of the P component for saturation coverage is $\sim 1.8\pm 0.2$ eV away from the other two components, which is consistent with the observation of a peak in electron-energy-loss spectra for a saturated Si(100) 2×1 -K surface by Tochiyama and Murata.²⁶

Angle-resolved normal emission spectra of the Si(100) valence band are shown in Fig. 5 for increasing K depositions. The lowermost spectrum was recorded on the

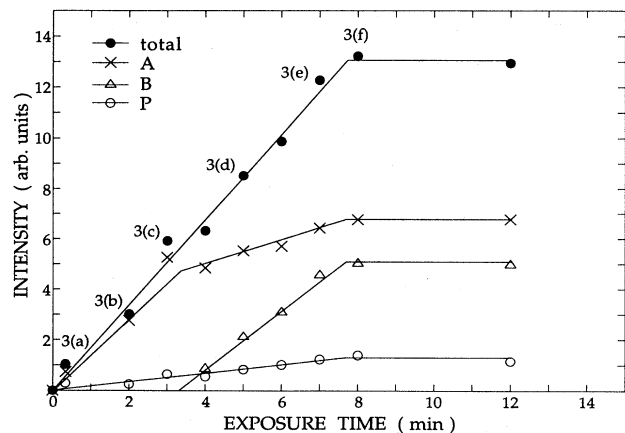


FIG. 4. K 3*p* integrated intensity versus the K exposure time. The labels are explained in the text.

clean Si(100) 2×1 surface. For small K exposures a clear peak F1 showed up at the Fermi level. The intensity of peak F1 grew with further adsorption of K and reached its maximum at $\Delta\Phi \approx -0.8$ eV. Larger K exposures resulted in a lower intensity and the structure F1 was no longer detectable for $\Delta\Phi = -1.65$ eV (not shown). The dangling-bond structures A and B of the clean surface were still observable for the smaller K coverages. As the K coverage increased the spectra became broader which made it difficult to discern the different structures. Close to saturation coverage two K-induced states C1 and C2 are resolved in the spectra. The uppermost spectrum ($\Delta\Phi = -3.51$ eV), which corresponds to saturation coverage, shows an overall downward shift by ~ 0.2 eV in agreement with the core-level results and it is related to the appearance of a weak feature F2 at the Fermi level. A weak third structure C3 is observed between the C1 and C2 structures. The whole series of valence-band spectra is very similar to another photoemission study of a *p*-type ($\rho = 20\text{--}40$ Ωcm) sample.²⁷

From the above experimental results the following picture of the K/Si(100) 2×1 system emerges. The strong peak F1 (Fig. 5) for the initial coverages is interpreted as due to a partial occupation of an empty surface band by the K 4*s* electrons. The population of the empty band leads to the abrupt shift of the Fermi-level pinning posi-

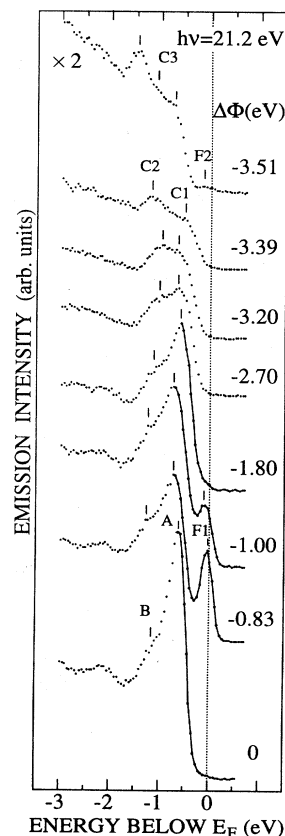


FIG. 5. Normal-emission valence-band spectra of Si(100) for increasing K coverage. The coverage was determined indirectly by measuring the work-function change.

tion. This is in analogy with the situation for clean and highly *n*-type doped samples where the *F*1 state is populated due to the presence of extra doping electrons.^{28,29} A donation of K 4*s* electrons to an empty surface band is consistent with the ionic bonding character reported for low coverages by low-energy ion-scattering spectroscopy.^{21,22}

The smeared out appearance of the Si 2*p* core-level spectra, for the smaller K exposures, indicates the existence of several shifted surface components which are likely to correspond to an inhomogeneous surface. Evidence for disorder on the surface, for the smaller coverages, has also been provided by STM studies of the K/Si(100) surface. The surface structure, as observed by STM, was found to be different in the vicinity of the adsorbed K atoms.^{15–19}

The increased sharpness of the Si 2*p* spectrum at $\sim \frac{1}{3}$ of θ_s ($\Delta\Phi = -2.65$ eV) most likely reflects an ordering of the surface. A mixed 2×1 and 2×3 LEED pattern was observed for a coverage at which the sharpening of the Si 2*p* spectrum had just occurred, which is in agreement with some experimental studies which have reported the observation of a 2×3 LEED pattern²⁰ as well as a 2×3 reconstruction from STM images^{15,16} in this coverage region.

At saturation coverage the line shape of the Si 2*p* core level becomes considerably sharper. A detailed analysis of the Si 2*p* spectra is presented in Fig. 6 and it will be discussed later. At RT saturation the intensity of the second K 3*p* component (*B*) is about 74% of component *A* (Fig. 3). Under the assumption that the largest K 3*p* component corresponds to a coverage of 0.5 ML one obtains a saturation coverage ~ 0.9 ML, at the most, which implies that the K double layer is not fully developed on the whole surface at saturation. This is consistent with the observation of a noncompleted double-layer structure.^{2,13}

As can be observed in Figs. 2, 3, and 5, the second abrupt energy shift by ~ 0.2 eV toward higher binding energy occurred when the surface got saturated. The shift seems to be caused by the occupation of a metallic state at the Fermi level observed as a weak feature *F*2 in Fig. 5, as previously shown in inverse and direct photoemission studies.¹²

The data in Figs. 6 and 7 show high-resolution Si 2*p* spectra with well-resolved surface shifts which allow us to derive quantitative information by a least-squares fitting procedure. An integrated background is used in the fitting procedure and the spin-orbit split, branching ratio and Lorentzian width were 0.602 eV, 0.475 ± 0.025 , and 0.07 eV (FWHM), respectively. Figure 6 shows fits to Si 2*p* spectra recorded at a photon energy of 130 eV. For a clean Si(100)2×1 surface, the Si atoms of the top-most layer form asymmetric dimers. A simple schematic illustration of a side view for this surface is shown as an inset in Fig. 6(a). As we presented in a previous paper²⁵ the two surface components *Su* and *Sd*, with binding-energy shifts of ~ -0.50 and ~ -0.08 eV, correspond to the up and down atoms of the asymmetric dimers. The Gaussian width (GW) for both components is 262 meV (FWHM). The second-layer component *D* (GW 246

meV) with a shift of ~ 0.21 eV and the fourth component *C* (GW 200 meV) located at ~ 0.20 eV to the right of the bulk component *B* (GW 170 meV) are also identified as in the previous study.²⁵ A recent theoretical calculation of surface core-level shifts on Si(100) by Pehlke and Scheffler is in good agreement with our results.³⁰ Figure 6(b) shows the Si 2*p* spectrum recorded on a saturated Si(100)2×1-K surface at room temperature. The most obvious change from the clean Si 2*p* spectrum is a big well-resolved component *S* (GW 235 meV) with an energy shift of ~ -0.42 eV on the low binding-energy side. Its intensity is approximately equal to the sum of the in-

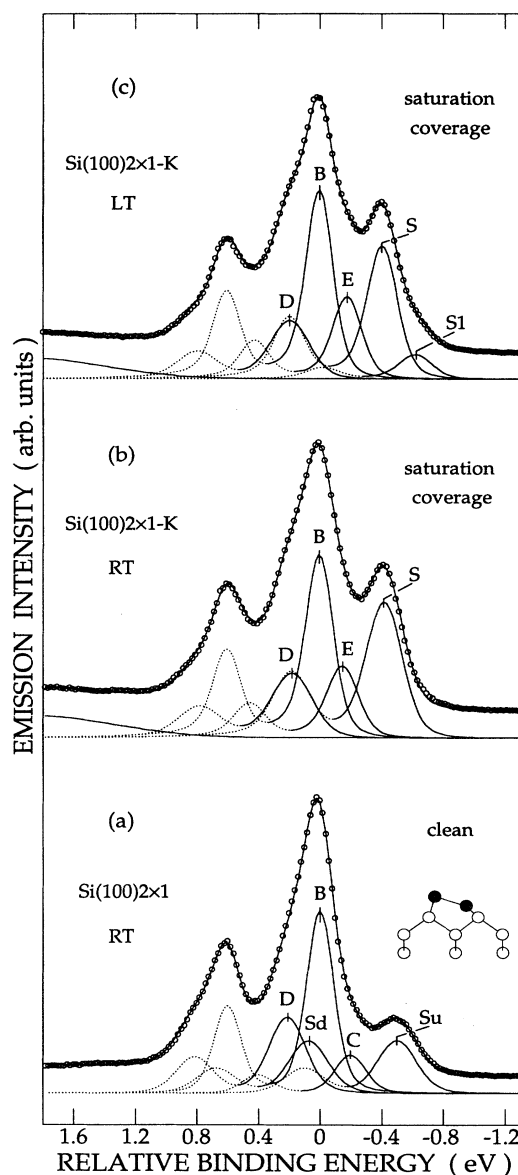


FIG. 6. Decomposed Si 2*p* core-level spectra recorded at normal emission with a photon energy of 130 eV. The solid and dotted lines represent the Si 2*p*_{3/2} and 2*p*_{1/2} parts, respectively. The solid curves through the data (circles) show the resulting fits.

tensities of components *Su* and *Sd* in spectrum 6(a) implying that *S* corresponds to approximately 1 ML of Si atoms. This is consistent with the presence of symmetric dimers on the surface in agreement with recent theoretical studies.^{10,11} The *C* and *D* components seem to have their counterparts also on the saturated Si(100)2×1-K surface. The *E* component (GW 200 meV), which exhibits an increased intensity compared to the *C* component of the clean surface, has a core-level shift of ~ -0.17 eV. The *D* component (GW 270 meV) is broader on the K saturated surface and it is located ~ 0.19 eV from the bulk Si 2*p* line. Spectrum 6(c) was recorded on the same surface as 6(b) but at ~ 100 K. The low temperature (LT)

was obtained by cooling the crystal with liquid nitrogen. Apart from being sharper, a small component *S1* (GW 210 meV) located at ~ -0.21 eV relative to component *S* (GW 190 meV) is observed in the spectrum. The increased background of the Si 2*p* spectra for the saturated Si(100)2×1-K surface in Figs. 6 and 7, especially 7(c), corresponds most likely to the overlayer plasmon-loss structure observed in the K 3*p* spectra. In addition, a singularity index for Doniach-Sunjić line shape of 0.05 is used for the K-saturated spectra in order to obtain a better fitting, while that is not necessary for the clean spectrum. The appearance of a more asymmetric line shape is consistent with the observation of a metallic character of the surface by several other experimental studies.^{12,15,16}

Further investigations of the nature of these components were made. Figure 7 shows Si 2*p* spectra recorded with different photon energies and emission angles for the same surface as that for spectrum 6(c). Spectrum 7(a) was recorded at normal emission with a photon energy of 115 eV; spectrum 7(b) is the same as spectrum 6(c); spectrum 7(c) was recorded at 60° emission with a photon energy of 130 eV. The spectra should, in principle, show an increasing surface sensitivity from 7(a)–7(c). All spectra are normalized with respect to the bulk component *B* so that one can easily see the changes in intensities of the other components with varying surface sensitivity. We obtained a small variation of the Gaussian width for each component for different surface sensitivities. For example, in spectrum 7(b), the Gaussian width of the bulk component *B* is 165 meV which drops to 145 meV in the most bulk-sensitive spectrum 7(a) and increases to 175 meV in the most surface-sensitive spectrum 7(c).

The most obvious structure *S* (GW ~ 180 meV) on the low binding-energy side of the spectra shows an increase in the intensity with higher surface sensitivity. The observed intensity of this component and the observation of a 2×1 LEED pattern leads naturally to the interpretation that the *S* component corresponds to symmetric Si dimers which nominally constitute 1 ML. The *S1* (GW ~ 200 meV) component that is visible in the LT spectrum in Fig. 6(c) may correspond to the up atoms of a small number of asymmetric dimers that still remain on the surface. Because of the slightly broader linewidth for the RT spectrum the small *S1* component does not show up in the raw data.

The structure exhibiting an increased intensity with larger surface sensitivity, on the high binding-energy side, is mainly due to the Si 2*p*_{1/2} part of the *D* component (GW ~ 240 meV). The specific variation of the *D* component with varying surface sensitivity suggests that it arises from the second layer in similarity with the clean Si(100) surface. The intensity of the *C* component (GW ~ 170 meV) varies only slightly between spectra of different surface sensitivity. This weak surface sensitivity suggests that *C* originates from subsurface layers.

The interpretation of the K 3*p* spectra for saturation coverage (Fig. 3) implies that the K double layer is not fully developed on the entire surface. Thus there seems to be a contradiction between the metallization observed with photoemission, inverse photoemission, and theoretic-

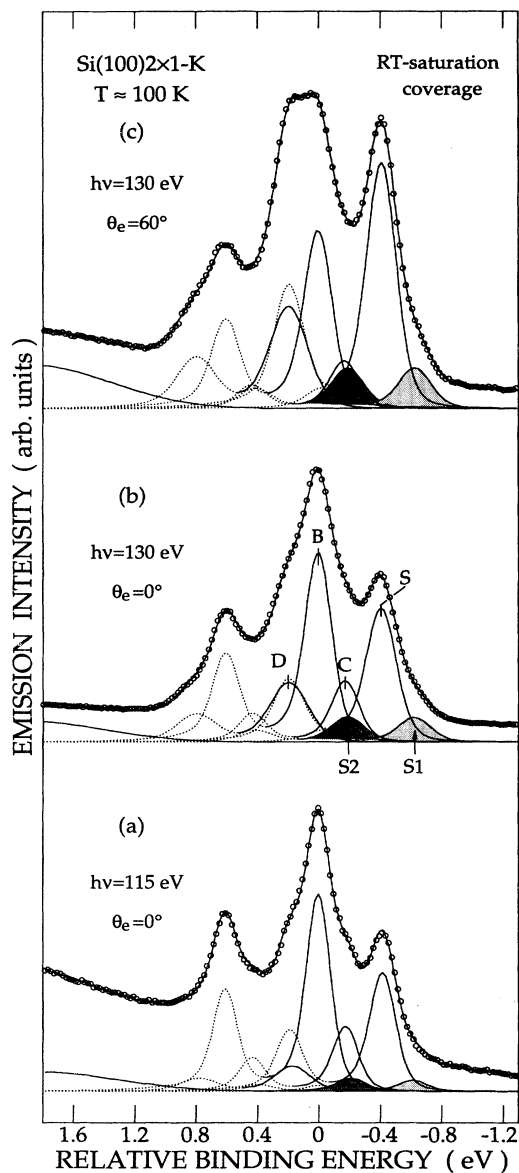


FIG. 7. Decomposed Si 2*p* core-level spectra obtained from the same surface as in Fig. 6(c) for two different photon energies and emission angles. The solid and dotted lines represent the Si 2*p*_{3/2} and 2*p*_{1/2} parts, respectively. The solid curves through the data (circles) show the resulting fits. The curve-fitting parameters and the labels are discussed in the text.

cal calculations based on a nominal 1 ML coverage, and the K 3*p* results suggesting a maximum coverage of ~0.9 ML at saturation. This discrepancy may be explained by the idea that the surface consists of large areas with a fully developed double-layer structure and minor areas with a noncompleted double-layer reconstruction. According to the theoretical work by Kobayashi *et al.*¹¹ and Morikawa *et al.*¹⁰ the Si dimers still remain slightly asymmetric on the surface with a coverage of 0.5 ML both for K atoms sitting on the “top” or the “trough” positions. The *S*1 component observed in our spectra might correspond to the up atoms of asymmetric Si dimers in smaller areas with a deficiency in the K coverage. A component corresponding to the down atom, with a higher binding energy compared to *S*1, can, however, not be identified in the raw data. It can be noted that, in Fig. 6, the intensity of the *E* component is higher for the Si(100)-K spectra compared to the *C* component of the clean spectrum which may be due to a contribution from a down-atom component close to the binding energy of the *C* component. In Fig. 7 we show fits to the spectra where we have included a component *S*2 (GW ~200 meV) corresponding to the down atoms of asymmetric dimers. Since this component cannot be directly identified in the spectra the position and intensity are, of course, speculative. Component *D* is interpreted as the contribution from the second Si layer in accordance with the clean Si(100)2×1 surface. If one models the saturated Si(100)2×1-K surface according to the result from the K 3*p* spectra, which suggests that ~74% of the area has a fully developed K double layer, and that the second K layer is missing on ~26% of the area, the ratio of the number of asymmetric and symmetric dimers would be about 0.35. This number is in fair agreement with the sum of the intensities of *S*1 and *S*2 divided by the intensity of *S*.

The results of our study provide a much more detailed picture of the Si(100)2×1-K surface than earlier studies involving Si and K core levels. We will here only compare with the results obtained by Riffe *et al.*¹⁴ since that is the only earlier study performed with a high experimental resolution. Despite the high energy resolution used by Riffe *et al.* their spectra look very broad which limits the value of a comparison and we thus concentrate on a few points. The raw Si 2*p* spectra obtained by Riffe *et al.* indicate that the intensity of the surface component on the low binding-energy side is higher for the saturated surface compared to the clean surface. This is in agreement with our finding that the *S* intensity is about twice the intensity of the *Su* component. Our *D* component, which we interpret as due to second-layer silicon atoms, was instead interpreted as the down-atom component of asymmetric dimers still present on the surface at saturation. From the results of the deconvolved Si 2*p* spectrum of the Si(100)2×1-K surface they concluded that about 50% of the Si dimers remain asymmetric. This is, how-

ever, partly based on their assumption that the up-atom component on the clean surface is split by the crystal field.³¹ As discussed in an earlier paper²⁵ we do not find any evidence for such crystal-field effects on either the Si(100)2×1 or Si(100)*c*(4×2) surfaces.

As we mentioned before, the K 3*p* spectra were recorded with photon energies of 130, 100, and 70 eV and they exhibit very similar results for exposure at room temperature. We find intensity ratios of the second component (dotted line, *B*, in Fig. 3) to the first component (solid line, *A*) in a range between ~0.70 and ~0.77 at saturation with the different photon energies. Since the variation in the intensity ratio obtained for different photon energies is rather small it is not very likely that the difference in the intensities of *A* and *B* is just due to diffraction effects. Even though diffraction effects should not be neglected we assign most of the difference in the intensity to a difference in the population of two types of sites on the surface.

IV. CONCLUSIONS

In summary, the K/Si(100)2×1-K system has been studied with high-resolution core-level spectroscopy and angle-resolved valence-band photoemission. A series of Si 2*p* and K 3*p* core-level and Si valence-band spectra for different K coverages has been analyzed. In the initial stage of K deposition, a surface state *F*1 appearing at the Fermi level leads to an abrupt change in the band bending by shifting the Fermi-level pinning position. At about $\frac{1}{3}$ of the saturation coverage, the Si 2*p* core-level spectra become sharper which probably reflects a higher degree of order associated with the appearance of the 2×3 structure. With further deposition, evidence for K adsorption at two different sites is obtained. The saturation coverage of K atoms was estimated to be ~0.9 of a monolayer at the most. A well-resolved surface component in the Si 2*p* core-level spectra together with a good 2×1 LEED pattern, both at RT and LT, suggest that K-modified symmetric Si dimers were formed on the major parts of the surface. Finally, a second abrupt change in the band bending on the surface was observed at saturation coverage, which is interpreted as a shift in the Fermi-level position caused by the onset of the occupation of an empty surface state. By considering the need for a larger singularity index for the Doniach-Sunjić line shape for both the Si 2*p* and K 3*p* spectra and the presence of a weak structure at the Fermi level, the metallic character of the saturated Si(100)2×1-K surface is confirmed in our study.

ACKNOWLEDGMENTS

The assistance of the MAX-laboratory staff is gratefully acknowledged. This work was supported by the Swedish Natural Science Research Council.

¹*Metallization and Metal-Semiconductor Interfaces*, Vol. 195 of NATO Advanced Study Institute, Series B: Physics, edited by I. P. Batra (Plenum, New York, 1989).

²E. G. Michel, P. Pervan, G. R. Castro, R. Miranda, and K.

Wandelt, Phys. Rev. B **45**, 11 811 (1992).

³J. D. Levine, Surf. Sci. **34**, 90 (1973).

⁴Y. Enta, T. Kinsohita, S. Suzuki, and S. Kono, Phys. Rev. B **36**, 9801 (1987).

- ⁵T. Abukawa and S. Kono, *Phys. Rev. B* **37**, 9097 (1988).
- ⁶S. Tanaka, N. Takagi, N. Minami, and M. Nishijima, *Phys. Rev. B* **42**, 1868 (1990).
- ⁷T. Makita, S. Kohmoto, and A. Ichimiya, *Surf. Sci.* **242**, 65 (1991).
- ⁸A. J. Smith, W. R. Graham, and E. W. Plummer, *Surf. Sci. Lett.* **243**, L37 (1991).
- ⁹D. Huang and P. R. Antoniewicz, *Phys. Rev. B* **44**, 9076 (1991).
- ¹⁰Y. Morikawa, K. Kobayashi, K. Terakura, and S. Blügel, *Phys. Rev. B* **44**, 3459 (1991).
- ¹¹K. Kobayashi, Y. Morikawa, K. Terakura, and S. Blügel, *Phys. Rev. B* **45**, 3469 (1992).
- ¹²L. S. O. Johansson and B. Reihl, *Phys. Rev. Lett.* **67**, 2191 (1991).
- ¹³M. C. Asensio, E. G. Michel, J. Alvarez, C. Ocal, R. Miranda, and S. Ferrer, *Surf. Sci.* **211/212**, 31 (1989).
- ¹⁴D. M. Riffe, G. K. Wertheim, J. E. Rowe, and P. H. Citrin, *Phys. Rev. B* **45**, 3532 (1992).
- ¹⁵U. A. Effner, D. Badt, J. Binder, T. Bertrams, A. Brodde, Ch. Lunau, H. Neddermeyer, and M. Hanbücken, *Surf. Sci.* **277**, 207 (1992).
- ¹⁶A. Brodde, Th. Bertrams, and H. Neddermeyer, *Phys. Rev. B* **47**, 4508 (1993).
- ¹⁷P. Soukiassian, J. A. Kubby, P. Mangat, Z. Hurych, and K. M. Schirm, *Phys. Rev. B* **46**, 13 471 (1992).
- ¹⁸T. Hashizume, Y. Hasegawa, I. Sumita, and T. Sakurai, *Surf. Sci.* **246**, 189 (1991).
- ¹⁹T. Hashizume, I. Sumita, Y. Murata, S. Hyodo, and T. Sakurai, *J. Vac. Sci. Technol. B* **9**, 742 (1991).
- ²⁰Y. Sasaki, Y. Enta, S. Suzuki, and S. Kono, *Surf. Sci.* **276**, 205 (1992).
- ²¹R. Souda, W. Hayami, T. Aizawa, and Y. Ishizawa, *Phys. Rev. B* **47**, 9917 (1993).
- ²²R. Souda, W. Hayami, T. Aizawa, and Y. Ishizawa, *Phys. Rev. B* **48**, 17 255 (1993).
- ²³A. Ishizaka and Y. Shiraki, *J. Electrochem. Soc.* **133**, 666 (1986).
- ²⁴L. S. O. Johansson, R. I. G. Uhrberg, P. Mårtensson, and G. V. Hansson, *Phys. Rev. B* **42**, 1305 (1990).
- ²⁵E. Landemark, C. J. Karlsson, Y.-C. Chao, and R. I. G. Uhrberg, *Phys. Rev. Lett.* **69**, 1588 (1992).
- ²⁶H. Tochihara and Y. Murata, *Surf. Sci. Lett.* **215**, L323 (1989).
- ²⁷Y. Enta, T. Kinoshita, S. Suzuki, and S. Kono, *Phys. Rev. B* **39**, 1125 (1989).
- ²⁸P. Mårtensson, A. Cricenti, and G. V. Hansson, *Phys. Rev. B* **33**, 8855 (1986).
- ²⁹J. E. Northrup, *Phys. Rev. B* **47**, 10 032 (1993).
- ³⁰E. Pehlke and M. Scheffler, *Phys. Rev. Lett.* **71**, 2338 (1993).
- ³¹G. K. Wertheim, D. M. Riffe, J. E. Rowe, and P. H. Citrin, *Phys. Rev. Lett.* **67**, 120 (1991).